Published in final edited form as:
Arch Ophthalmol. 2008 June ; 126(6): 765–771. doi:10.1001/archopht.126.6.765.

Detailed Visualization of the Anterior Segment Using Fourier-Domain Optical Coherence Tomography

Sanjay Asrani, MD, **Marinko Sarunic, PhD**, **Cecilia Santiago, MD**, and **Joseph Izatt, PhD**
Duke University Eye Center (Drs Asrani and Santiago) and Department of Biomedical Engineering (Drs Sarunic and Izatt), Duke University, Durham, North Carolina

Abstract

Objective—To study details of the anterior chamber drainage angle using Fourier-domain optical coherence tomography in healthy subjects and patients with angle abnormalities.

Methods—A high-speed anterior segment optical coherence tomography prototype was developed using a 1310-nm-wavelength swept light source. Six healthy subjects and 6 patients with glaucoma were imaged in an observational cross-sectional study.

Results—Schlemm's canal and the trabecular meshwork were visualized in all of the patients. Fifteenmillimeter scans enabled entire anterior segment visualization providing configuration details of the iris with respect to the angle. Four-millimeter scans permitted detailed views of the angle configuration and its structures. Volumetric imaging was possible and Schlemm's canal was visualized along part of its circumference.

Conclusion—Anterior segment Fourier-domain optical coherence tomography permits detailed noncontact imaging of the angle and its structures, providing a tool to improve our understanding of the pathogenesis of narrow-angle glaucoma.

VISUALIZATION OF THE TRA-becular meshwork and Schlemm's canal could be a valuable tool for glaucoma diagnosis and treatment, but it requires resolution in the range of tens of micrometers. Optical coherence tomography (OCT) is an emerging noncontact, noninvasive imaging modality for cross-sectional imaging of biological tissue.[1] A time-domain (TD) OCT system operating at a wavelength of 1310 nm and a line rate of 2 kHz has been commercialized for ocular anterior segment imaging (Visante OCT; Carl Zeiss Meditec, Dublin, California). Narrow anterior chamber angles have been studied using a prototype TDOCT imaging system.[2,3] Optical coherence tomography was found to be a promising method for screening individuals at risk for narrow-angle glaucoma, providing higher resolution than ultrasound biomicroscopy with the additional advantages of a noncontact imaging modality compatible with slitlamp biomicroscopy observation. However, Schlemm's canal and the trabecular meshwork have not been readily visualized with the existing TDOCT systems.[4]

Optical coherence tomography has been revolutionized in recent years by the development of Fourier-domain (FD) techniques, which provide a substantial increase in sensitivity over

Correspondence: Sanjay Asrani, MD, Duke University Eye Center, Box 3802, Durham, NC, 27710 (asran002@mc.duke.edu)..
Previous Presentation: This study was presented at the annual meeting of the American Glaucoma Society; March 4, 2006; Charleston, South Carolina.
Additional Contributions: Kevin Hsu, PhD, Micron Optics, Inc, loaned the high-speed swept laser source, and Bioptigen, Inc, supplied the base software package for acquisition and display.

Financial Disclosure: Drs Sarunic and Izatt are inventors of intellectual property, assigned to Duke University, related to the subject of this article. Dr Izatt is a founder and part-time employee of Bioptigen, Inc.

traditional TDOCT systems.[5-7] This increase in sensitivity has been used to image at high scan rates without increasing the optical exposure or sacrificing image brightness. However, high-speed FDOCT systems operating at a central wavelength of 1310 nm have been limited in useful imaging depths to less than 3 or 4 mm,[8-12] hindering ocular anterior segment imaging. Images of the anterior chamber, the depth of which typically spans greater than 4 mm, are corrupted by a symmetric overlapping artifact, referred to in the literature as the complex conjugate artifact,[5-7] that obstructs important physiological details. A doubling of the image depth can be achieved by resolving the complex conjugate artifact using various methods,[13-24] thus permitting full-range imaging. A subset of these depth-doubling techniques has been previously applied for technology demonstrations of full-depth imaging of the anterior segment.[10-16,21-23]

In this article, we describe a pilot study of high-speed, high-resolution imaging of the ocular anterior segment in vivo using a swept-source FDOCT system. Full-range imaging is provided using a 3×3 fiber coupler topology and quadrature projection processing as described in detail elsewhere.[24] In addition to imaging of the drainage angle region and iris, the FDOCT system permits visualization of Schlemm's canal and the trabecular meshwork. Both 2-dimensional and volumetric cross-sectional images are shown, suggesting a wide range of potential clinical applications.

METHODS

This study was approved by the institutional review board of Duke University Medical Center. Following informed consent, healthy subjects and patients with glaucoma were recruited. Six subjects were healthy volunteers who were recruited from among the staff of the university. They ranged from 26 to 50 years in age. They had no family history of glaucoma, no history of raised intraocular pressure or ocular trauma, and normal ophthalmic examination results with gonioscopy revealing an angle open to grade III or grade IV by the Shaffer method (angle between the trabecular meshwork and iris>20°). Patients with myopia or hypermetropia more than ±3 diopters were excluded.

Six patients with narrow-angle glaucoma were recruited from the glaucoma service of Duke University Eye Center. They were selected for the study if their gonioscopy revealed angles of grade II, I, slit, or 0 by the Shaffer method, they had a history of raised intraocular pressure, and they either were receiving treatment with medications or were scheduled for or already had peripheral laser iridotomy performed. Four patients had primary narrow-angle glaucoma and 2 patients had secondary narrow-angle glaucoma.

The images were acquired using the novel full-range FDOCT system discussed elsewhere.[23] The average optical exposure on the eye was 3.75 mW from a 1310-nm-wavelength swept source (Micron Optics, Inc, Atlanta, Georgia), well within the American National Standards Institute limit of 15.4 mW for continuous exposure at this wavelength.[25] The FDOCT system was integrated into a modified slitlamp biomicroscope for ease of patient alignment, requiring only a few seconds. The estimated system resolution was 9 μm axially (in air) determined by the source bandwidth and 19 μm laterally defined as the full width at half maximum of the sample arm beam. The full-range images were acquired, processed, and displayed in real time using custom software (base package provided by Bioptigen Inc, Durham, North Carolina) on a dual-core Pentium desktop computer. High-resolution 2-dimensional B-scans comprising 800 A-scans per B-scan were acquired at 6.7 frames per second and viewed in a real-time display mode. Volumetric imaging required a faster frame rate and the number of lines per frame was reduced to 400, resulting in an acquisition speed of 13.4 B-scans per second. Volumes consisting of 60 elevation frames were acquired in 4.5 seconds. The line scan across the anterior segment was most commonly performed horizontally to prevent interference from

the eyelids. A few vertical scans were performed with the upper eyelid having to be retracted by the patient.

RESULTS

Full-range FDOCT imaging of the entire anterior chamber width demonstrated the iris configuration with respect to the anterior lens surface. In 1 of the healthy subjects with myopia, a concave iris was detected on FDOCT and confirmed on clinical examination (Figure 1). No clinical evidence of pigment dispersion was detected. In the high-resolution 4-mm scans of the angle region, the configuration of Schlemm's canal was visible along with the trabecular meshwork in eyes of healthy subjects (Figure 2A and B). The trabecular meshwork was seen as a triangular structure with the base attached at the scleral spur. The scleral spur was identified by its peaked outline and the slight projection into the anterior chamber (Figure 2C). Schlemm's canal was seen as a curvilinear lucent area external to the trabecular meshwork. This lucent area extended from the scleral spur to the anterior tip of the trabecular meshwork located at the end of the Descemet membrane. This lucent area corresponding to Schlemm's canal was distinct from the lucency of the corneal stroma. Although the ciliary body outline was visible in FDOCT images, details of the ciliary processes were not visible (Figure 2B). The gonioscopic appearance of the angle in the healthy subject shown in Figure 1 was open to the ciliary body band (grade IV by the Shaffer method; the angle between the iris and trabecular meshwork was 45°) and the 4-mm FDOCT scan demonstrated the cross-sectional view of the same in Figure 3A. In another healthy subject, gonioscopy revealed the angle to be open to the scleral spur (grade III by the Shaffer method; the angle between the iris and trabecular meshwork was < 45° but > 20°); its cross-sectional view is shown in Figure 3B.

Representative quantitative measurement was performed in a patient with gonioscopic grade II narrow-angle glaucoma. The angle opening distance at 500 μm (AOD500) is the length of a perpendicular from a corneal endothelial point 500 μm anterior to the scleral spur drawn to the iris. The angle recess area at 500 μm (ARA500) is the triangular area enclosed by the AOD500, the line along the corneal endothelium from the scleral spur to the AOD500, and the line following the contour of the iris from the scleral spur to the AOD500. The boundaries of the epithelium, endothelium, and iris were traced in raw coordinates manually. These lines were then converted to processed coordinates accounting for the refraction at each interface according to Snell's law. The AOD500 (308 μm) and ARA500 (0.11 mm^2) measurements were performed in processed coordinates from these boundary-delineating lines (Figure 4). The 2 measurements have been described previously using TDOCT.[2] Our measurements of AOD500 and ARA500 agree with the previously reported measurements and are within the range of values reported for narrow angles.[2,23]

Among the patients with narrow-angle glaucoma, 4 had primary narrow-angle glaucoma. In 1 patient, the right eye was examined before laser peripheral iridotomy for a potentially occludable narrow angle. Gonioscopy showed the angle to be narrow (grade I) with the anterior trabecular meshwork visible. The high-resolution FDOCT scan in the angle region demonstrated the extremely narrow space between the root of the iris and the trabecular meshwork (Figure 5A and B). In another patient, gonioscopy demonstrated the angle graded as 0. No angle structures were visible. The FDOCT scan shows the near touch between the trabecular meshwork and the root of the iris (Figure 5C and D). A patient with a clinical diagnosis of plateau iris who had episodes of high intraocular pressure and colored halos around lights despite a patent laser peripheral iridotomy was found to have a narrow angle (grade I) with the anterior trabecular meshwork visible on slitlamp gonioscopy. The FDOCT scan demonstrated a narrow space between the trabecular meshwork and the root of the iris when the room lights were on. This space was obliterated (resulting in a closed angle) when the room lights were switched off, and it returned to its narrow configuration once the room lights were

turned on again (Figure 6). Although the ciliary body outline was visible in FDOCT images, details of the ciliary processes were not visible. In the fourth patient with narrow-angle glaucoma, scattered peripheral anterior synechiae were visible on gonioscopy. Areas of adhesion were observed between the root of the iris and the trabecular meshwork in the FDOCT cross-sectional image (Figure 7).

Volumetric imaging was performed by acquiring data sets consisting of 1024×400×60 pixels (axial×lateral ×elevation) in 4.5 seconds. The images were rendered using 3DView (RMR Systems, Suffolk, England), which limited the number of displayed pixels to 512. Cross-sectional planes of a volumetric image of a normal anterior segment are shown in Figure 8 and were acquired with the scan width reduced to 7 mm. Schlemm's canal was visualized along part of the circumference by removing the overlying layers in the rendered 3-dimensional image. Additional information may be gleaned from the volumetric rendering by examining cross sections through the data set. A patient with secondary glaucoma due to a ciliary body tumor was also imaged. A volume scan was performed (Figure 9), and it showed the elevation of the peripheral iris in the inferior region of the eye causing a shallowing of the anterior chamber. However, the limited depth penetration of the FDOCT prevented imaging of the actual tumor located beneath the iris. Figure 10 shows the image from a patient with narrow-angle glaucoma secondary to a multiloculated iris cyst that is visible in the iris pigment epithelium.

COMMENT

In this study we have demonstrated, to our knowledge for the first time, high-resolution, noncontact, in vivo imaging of the anterior segment, trabecular meshwork, and Schlemm's canal using a full-range FDOCT system. The axial resolution using the FDOCT system was less than 9 μm as compared with more than 11 μm with TDOCT.[2,3] Resolution of the complex conjugate artifact permitted a scan depth in excess of 6.3 mm, allowing imaging of the entire depth of the anterior chamber while reducing artifacts. The reduced resolution observed in some of the images was introduced by imperfect sampling by the prototype wavelength swept interferometric system and was not an artifact of the complex conjugate-resolved imaging algorithm. High-resolution images (consisting of 1024 axial points by 800 lateral lines) provided a view of the trabecular meshwork and Schlemm's canal. We have demonstrated the ability to view the structural relationship between the periphery of the iris and the trabecular meshwork as well as the visualization of peripheral anterior synechiae. Detailed imaging may help to improve understanding of the patho-genesis of pupillary block syndrome,[24] plateau iris syndrome, and possibly malignant glaucoma.

Visualization of the angle nasally and temporally along a line that horizontally crosses the pupil provides data about the angle across only 2 points along the circumference. This typically may represent the overall nature of the angle as seen gonioscopically in most cases. However, there are eyes with uneven angle configuration as they progress from having open to narrow angles. To visualize the angle and Schlemm's canal along the entire circumference, volumetric scans may be useful. Volumetric scanning was possible with the FDOCT system at 13.4 frames per second (thus minimizing motion artifact), which is useful for quantitative measurements of the anterior chamber in 3 dimensions. Variations in the depth of the anterior chamber such as in the case of the eye with a ciliary body tumor can be easily visualized with the help of volumetric scanning. However, it is important to note that FDOCT was unable to image the ciliary processes or structures beneath the pigmented layer of the iris.

Proper gonioscopy to observe the configuration of the angle of the anterior chamber requires a learned skill that involves recognition of the landmarks of the angle with and without compression by the contact gonioscopic lens. Recognition of landmarks can be challenging

during gonioscopy on eyes with minimal pigmentation in their trabecular meshwork. However, even with proper technique, gonioscopy requires the use of slitlamp illumination, which typically causes pupillary constriction. Constriction of the pupil causes the iris to be drawn away from the angle and may thus artificially open up a very narrow angle. Compression caused by inadvertent pressure by the examiner holding the lens during gonioscopy can also falsely open the angle. This may lead to an erroneous diagnosis of an open angle with the potential for major clinical consequences, resulting in an acute angle-closure glaucoma or chronic angle closure. The incidence of both of these types of glaucoma may be reduced if narrow angles are correctly identified and prophylactic laser iridotomy is performed before any synechial formation occurs.

A noncontact OCT system that operates in the infrared spectrum permits viewing of the angle in its natural state without pressure from a contact lens or the effects of illumination.[23] Because details of the trabecular meshwork are visible with the FDOCT system, the triangular space between the root of the iris and the trabecular meshwork can be evaluated for the relative position of the root of the iris with regard to the corneoscleral bands of the trabecular meshwork. Widespread application of anterior segment FDOCT to glaucoma may permit accurate diagnosis even by a general eye care practitioner without training in gonioscopy. This may aid in the diagnosis of angle closure, in both acute and chronic states, which constitutes one-half of the total glaucoma cases in the world.[26]

Numerous studies have investigated the structures of the trabecular meshwork and Schlemm's canal, resulting in better understanding of their microscopic and molecular composition. These structures have been studied using either histopathological examination or perfusion studies of postmortem specimens.[27-29] Despite these studies on the outflow system, our knowledge has been limited owing to the lack of a noninvasive imaging system that permits visualization of these structures in vivo. Imaging by FDOCT may permit studies to detect changes of the trabecular meshwork and Schlemm's canal with accommodation, with different pharmacological agents, and following surgery. Detailed imaging of Schlemm's canal may also help in understanding the pathogenesis and evolution of open-angle glaucoma.

Nonpenetrating glaucoma surgical procedures have not yet been widely adopted secondary to the high skill level required to identify Schlemm's canal and thus long surgical times.[30-32] Each of these surgical procedures is heavily dependent on precise localization of Schlemm's canal. Adapting the FDOCT system to the operative microscope may allow intraoperative visualization of Schlemm's canal, permitting easier, more accurate, and more efficient surgery on the canal.[4] Volumetric scanning can also aid in the study of patients who have undergone surgical procedures such as viscocanalostomy and deep sclerectomy by cross-sectional image evaluation in different planes. This may permit study of multiple parameters, for example, the extent of the spread of the viscoelastic along the circumference of Schlemm's canal or the state of the Descemet window.

The limitations of TD systems include image degradation due to motion artifact secondary to patient's microsaccades. The fast scan rate of 13.4 frames per second for FDOCT allows real-time cross-sectional imaging at high resolution and thus may permit image-guided interventions such as injections into Schlemm's canal. Intraoperative FDOCT imaging may permit development of precise and targeted glaucoma surgery such as removal of the trabecular meshwork using the trabectome.[33] Imaging may also aid in the placement of transcanalicular shunts (microtube shunt; Glaukos Corp, Laguna Hills, California), which enable aqueous humor to bypass the trabecular meshwork.[34] Various pharmacotherapeutic treatments such as gene transfer to the trabecular meshwork could potentially be injected directly into Schlemm's canal using FDOCT imaging to guide the needle.

In summary, anterior segment FDOCT may assist in understanding the pathogenesis of different types of glaucoma, aid in accurate diagnosis, and provide new avenues of treatment.

Funding/Support

This work was supported in part by an unrestricted grant from Research to Prevent Blindness, Inc, and by grant EY013516 from the National Eye Institute. Dr Asrani is a recipient of the Career Development Award from Research to Prevent Blindness, Inc.

REFERENCES

1. Huang D, Swanson EA, Lin CP, et al. Optical coherence tomography. Science 1991;254(5035):1178–1181. [PubMed: 1957169]
2. Radhakrishnan S, Goldsmith J, Huang D, et al. Comparison of optical coherence tomography and ultrasound biomicroscopy for detection of narrow anterior chamber angles. Arch Ophthalmol 2005;123(8):1053–1059. [PubMed: 16087837]
3. Radhakrishnan S, Huang D, Smith SD. Optical coherence tomography imaging of the anterior chamber angle. Ophthalmol Clin North Am 2005;18(3):375–381. [PubMed: 16054995]
4. Geerling G, Muller M, Winter C, et al. Intraoperative 2-dimensional optical coherence tomography as a new tool for anterior segment surgery. Arch Ophthalmol 2005;123(2):253–257. [PubMed: 15710824]
5. Leitgeb R, Hitzenberger CK, Fercher AF. Performance of fourier domain vs time domain optical coherence tomography. Opt Express 2003;11(8):889–894. [PubMed: 19461802]
6. de Boer JF, Cense B, Park BH, Pierce MC, Tearney GJ, Bouma BE. Improved signal-to-noise ratio in spectral-domain compared with time-domain optical coherence tomography. Opt Lett 2003;28(21):2067–2069. [PubMed: 14587817]
7. Choma MA, Sarunic MV, Yang C, Izatt JA. Sensitivity advantage of swept source and Fourier domain optical coherence tomography. Opt Express 2003;11(18):2183–2189. [PubMed: 19466106]
8. Yun SH, Tearney GJ, Bouma BE, Park BH, de Boer JF. High-speed spectral-domain optical coherence tomography at 1.3 μm wavelength. Opt Express 2003;11(26):3598–3604. [PubMed: 19471496]
9. Yun SH, Tearney GJ, de Boer JF, Iftimia N, Bouma BE. High-speed optical frequency-domain imaging. Opt Express 2003;11(22):2953–2963. [PubMed: 19471415]
10. Huber R, Wojtkowski M, Fujimoto JG. Fourier Domain Mode Locking (FDML): a new laser operating regime and applications for optical coherence tomography. Opt Express 2006;14(8):3225–3237. [PubMed: 19516464]
11. Christopoulos V, Kagemann L, Wollstein G, et al. In vivo corneal high-speed, ultra high-resolution optical coherence tomography. Arch Ophthalmol 2007;125(8):1027–1035. [PubMed: 17698748]
12. Yasuno Y, Madjarova VD, Makita S, et al. Three-dimensional and high-speed swept-source optical coherence tomography for in vivo investigation of human anterior eye segments. Opt Express 2005;13(26):10652–10664. [PubMed: 19503280]
13. Sarunic MV, Choma MA, Yang C, Izatt JA. Instantaneous complex conjugate resolved spectral domain and swept-source OCT using 3×3 fiber couplers. Opt Express 2005;13(3):957–967. [PubMed: 19494959]
14. Wojtkowski M, Kowalczyk A, Leitgeb R, Fercher AF. Full range complex spectral optical coherence tomography technique in eye imaging. Opt Lett 2002;27(16):1415–1417. [PubMed: 18026464]
15. Gotzinger E, Pircher M, Leitgeb RA, Hitzenberger CK. High speed full range complex spectral domain optical coherence tomography. Opt Express 2005;13(2):583–594. [PubMed: 19488388]
16. Targowski P, Gorczynska W, Szkulmowski M, Wojtkowski M, Kowalczyk A. Improved complex spectral domain OCT for in vivo eye imaging. Opt Commun 2005;249(13):357–362.
17. Bachmann AH, Leitgeb RA, Lasser T. Heterodyne Fourier domain optical coherence tomography for full range probing with high axial resolution. Opt Express 2006;14(4):1487–1496. [PubMed: 19503473]

18. Vakoc BJ, Yun SH, Tearney GJ, Bouma BE. Elimination of depth degeneracy in optical frequency-domain imaging through polarization-based optical demodulation. Opt Lett 2006;31(3):362–364. [PubMed: 16480209]
19. Yun SH, Tearney GJ, De Boer JF, Bouma BE. Removing the depth-degeneracy in optical frequency domain imaging with frequency shifting. Opt Express 2004;12(20):4822–4828. [PubMed: 19484034]
20. Zhang J, Nelson JS, Chen ZP. Removal of a mirror image and enhancement of the signal-to-noise ratio in Fourier-domain optical coherence tomography using an electro-optic phase modulator. Opt Lett 2005;30(2):147–149. [PubMed: 15675695]
21. Davis AM, Choma MA, Izatt JA. Heterodyne swept-source optical coherence tomography for complete complex conjugate ambiguity removal. J Biomed Opt 2005;10(6):064005. [PubMed: 16409070]
22. Kerbage C, Lim H, Sun W, Mujat M, de Boer JF. Large depth-high resolution full 3D imaging of the anterior segments of the eye using high speed optical frequency domain imaging. Opt Express 2007;15(12):7117–7125. [PubMed: 19547029]
23. Sarunic MV, Asrani S, Izatt JA. Imaging the ocular anterior segment with real-time, full-range Fourier-domain optical coherence tomography. Arch Ophthalmol 2008;126(4):537–542. [PubMed: 18413525]
24. Sarunic MV, Applegate BE, Izatt JA. Real-time quadrature projection complex conjugate resolved Fourier domain optical coherence tomography. Opt Lett 2006;31(16):2426–2428. [PubMed: 16880844]
25. American National Standards Institute. American National Standard for Safe Use of Lasers. Laser Institute of America; Orlando, FL: 2000. p. 45-49.ANSI Z 136.1-2000
26. Quigley HA, Broman AT. The number of people with glaucoma worldwide in 2010 and 2020. Br J Ophthalmol 2006;90(3):262–267. [PubMed: 16488940]
27. Allingham RR, de Kater AW, Ethier CR. Schlemm's canal and primary open angle glaucoma: correlation between Schlemm's canal dimensions and outflow facility. Exp Eye Res 1996;62(1):101–109. [PubMed: 8674505]
28. Johnson DH, Matsumoto Y. Schlemm's canal becomes smaller after successful filtration surgery. Arch Ophthalmol 2000;118(9):1251–1256. [PubMed: 10980771]
29. Rosenquist RC Jr, Melamed S, Epstein DL. Anterior and posterior axial lens displacement and human aqueous outflow facility. Invest Ophthalmol Vis Sci 1988;29(7):1159–1164. [PubMed: 3262095]
30. Johnson DH, Johnson M. How does nonpenetrating glaucoma surgery work? aqueous outflow resistance and glaucoma surgery. J Glaucoma 2001;10(1):55–67. [PubMed: 11219641]
31. Smit BA, Johnstone MA. Effects of viscoelastic injection into Schlemm's canal in primate and human eyes: potential relevance to viscocanalostomy. Ophthalmology 2002;109(4):786–792. [PubMed: 11927441]
32. Schuman JS, Chang W, Wang N, de Kater AW, Allingham RR. Excimer laser effects on outflow facility and outflow pathway morphology. Invest Ophthalmol Vis Sci 1999;40(8):1676–1680. [PubMed: 10393035]
33. Minckler DS, Baerveldt G, Alfaro MR, Francis BA. Clinical results with the Trabectome for treatment of open-angle glaucoma. Ophthalmology 2005;112(6):962–967. [PubMed: 15882909]
34. Bahler CK, Smedley GT, Zhou J, Johnson DH. Trabecular bypass stents decrease intraocular pressure in cultured human anterior segments. Am J Ophthalmol 2004;138(6):988–994. [PubMed: 15629290]

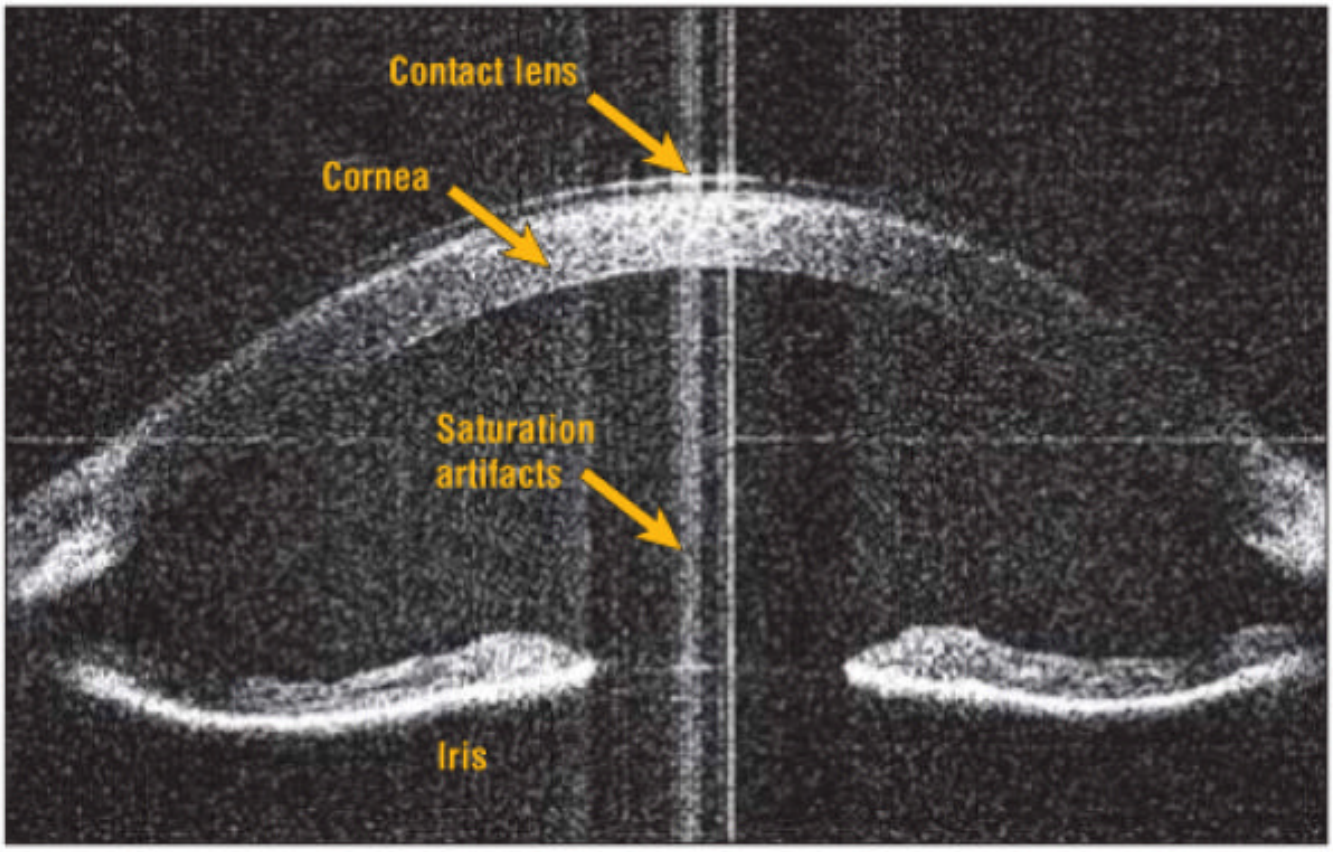

Figure 1.
Concave iris configuration seen in a patient with mild myopia. The full depth of the anterior chamber can be visualized.

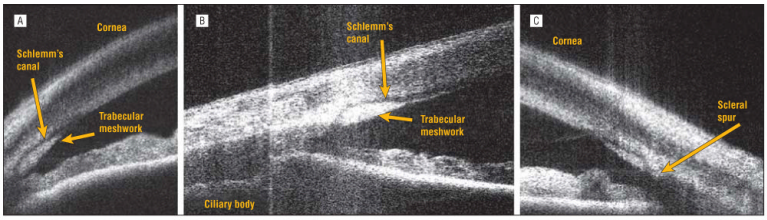

Figure 2.

Detailed angle structures. A, The trabecular meshwork is visible as a triangular body and Schlemm's canal as a curvilinear lucent space external to the trabecular meshwork. B, The ciliary body outline is visible along with Schlemm's canal and the trabecular meshwork in another eye of a healthy subject. C, Note the scleral spur as a structure projecting into the anterior chamber at the root of the trabecular meshwork.

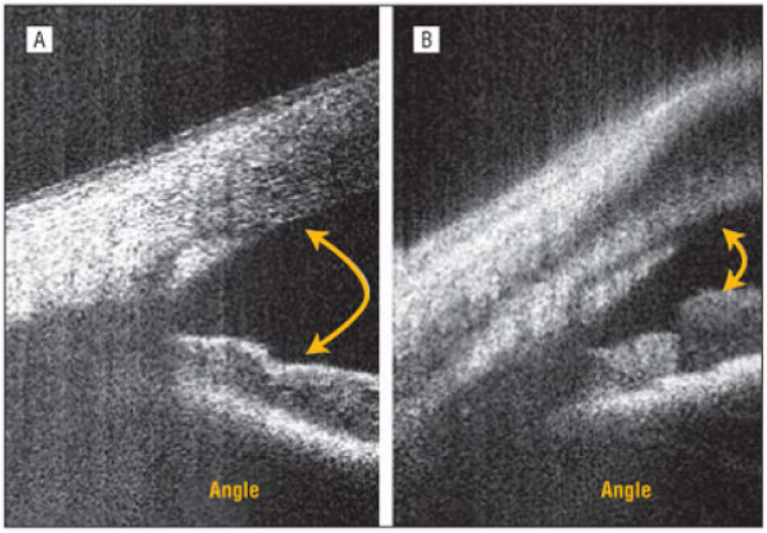

Figure 3.
Angle configurations. A, An eye clinically open to the ciliary body band on gonioscopy. B, An eye open to the scleral spur on gonioscopy.

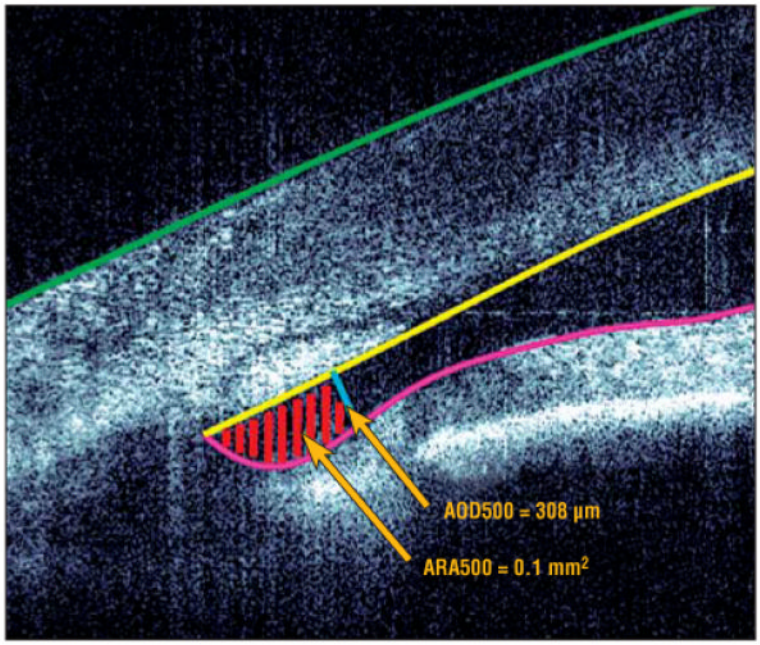

Figure 4.

Representative narrow angle measurement. The epithelium, endothelium, and iris were manually delineated in unprocessed coordinates. The angle opening distance at the 500-µm (AOD500) line is shown in blue, and the angle recess area at the 500-µm (ARA500) region is hatched with red lines in unprocessed coordinates. The values for the AOD500 and ARA500 were calculated in processed coordinates, and the ARA500 was obtained by integration of the equations describing the lines.

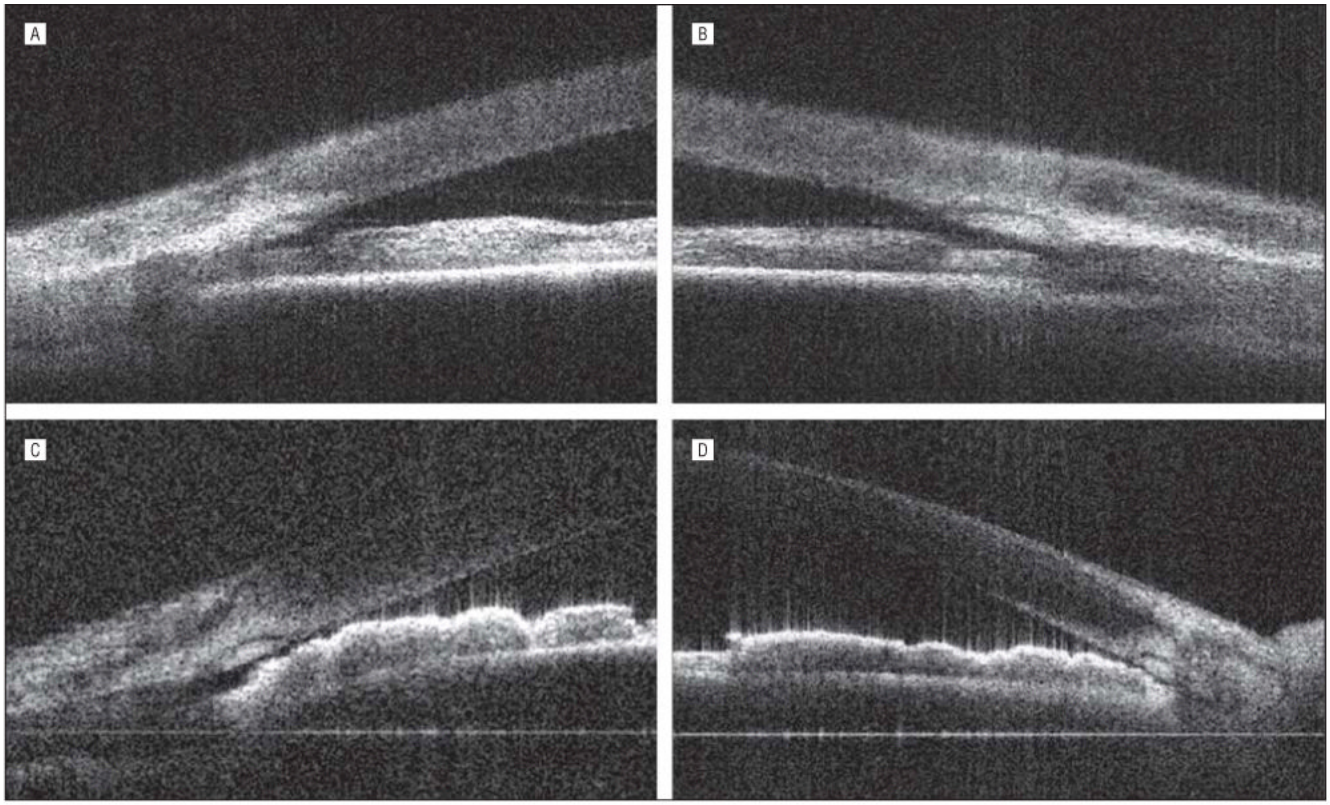

Figure 5.
High-resolution Fourier-domain optical coherence tomographic scans of narrow angles with gonioscopic grade I and grade 0. A, A very narrow space is visible between the root of the iris and the trabecular meshwork in the right eye of a patient with narrow-angle glaucoma (gonioscopic grade I). B, The left eye of the same patient (A) shows similar findings. C, Near touch between the trabecular meshwork and the root of the iris is visible in the right eye of another patient with narrow-angle glaucoma (gonioscopic grade 0). D, The left eye of the same patient (C) shows a similar angle configuration.

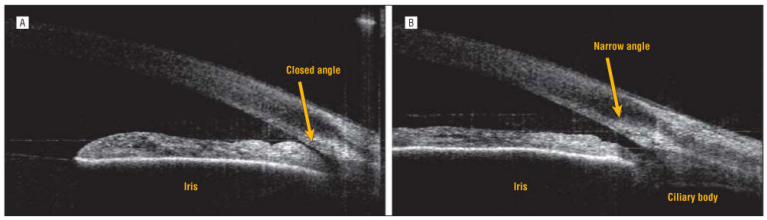

Figure 6.

Images with the room lights turned off (A) and back on (B). A, A closed angle with the iris root almost in approximation with the trabecular meshwork when the room lights are off. B, On turning the room lights on, the pupil constricts with ensuing stretching of the iris and widening of the angle.

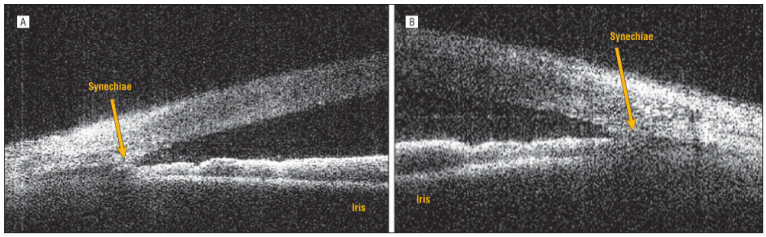

Figure 7.
Peripheral anterior synechiae in a patient with narrow-angle glaucoma. A, Adhesion between the iris root and the trabecular meshwork is visible in the right eye. B, Similar findings are seen in the left eye of the same patient.

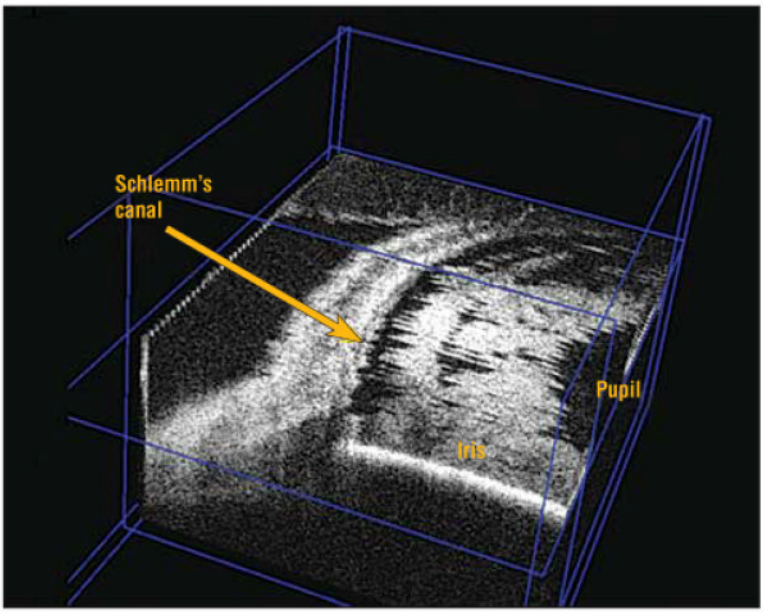

Figure 8.
Cross-sectional planes of a volumetric image of a normal anterior segment showing Schlemm's canal along part of the circumference by removing the overlying layers in the rendered 3-dimensional image.

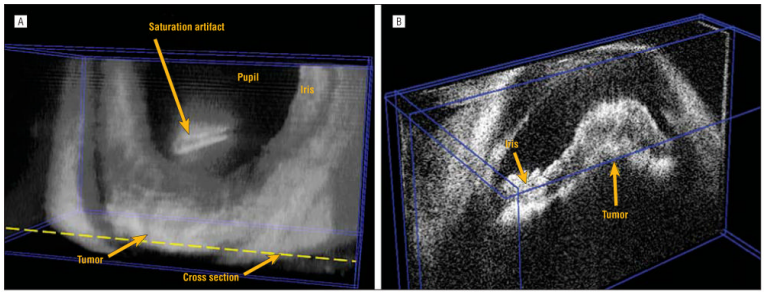

Figure 9.
An eye with a ciliary body tumor. A, A volumetric rendering showing irregularity of the anterior chamber depth due to elevation of the peripheral iris in the inferior region of the eye. B, A cross-sectional plane through the tumor location. Note that the actual tumor of the ciliary body is not visible.

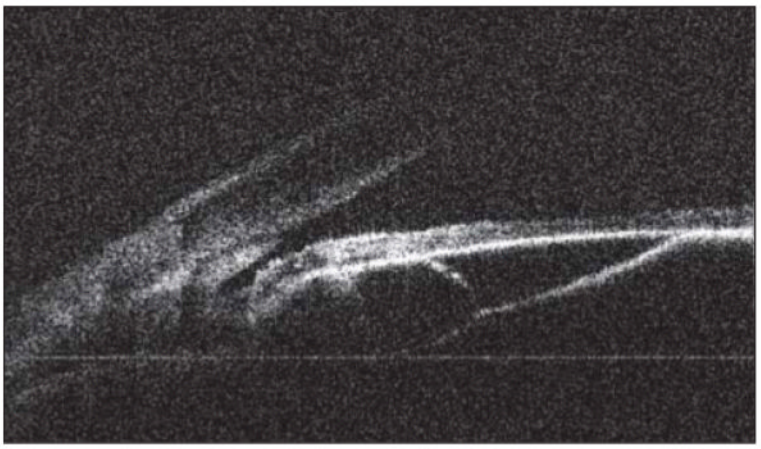

Figure 10.
Multiloculated iris cyst in the iris pigment epithelium.